Environ. Sci. Technol. **2005**, *39,* 5276−5284

On-Road Emission Rates of PAH and *n*-Alkane Compounds from Heavy-Duty Diesel Vehicles

SANDIP D. SHAH,[†,‡]
TEMITOPE A. OGUNYOKU,[†,‡]
J. WAYNE MILLER,[‡] AND
DAVID R. COCKER III*[,†,‡]

Department of Chemical and Environmental Engineering, University of California, Riverside, California 92521, and Center for Environmental Research and Technology (CE-CERT), Bourns College of Engineering, University of California, 1084 Columbia Avenue, Riverside, California 92507

This paper presents the quantification of the emission rates of PAH and *n*-alkane compounds from on-road emissions testing of nine heavy-duty diesel (HDD) vehicles tested using CE-CERT's Mobile Emissions Laboratory (MEL) over the California Air Resources Board (ARB) Four Phase Cycle. Per mile and per CO_2 emission rates of PAHs and *n*-alkanes were highest for operation simulating congested traffic (Creep) and lowest for cruising conditions (Cruise). Significant differences were seen in emission rates over the different phases of the cycle. Creep phase fleet average emission rates (mg mi^{-1}) of PAHs and *n*-alkanes were approximately an order of magnitude higher than Cruise phase. This finding indicates that models must account for mode of operation when performing emissions inventory estimates. Failure to account for mode of operation can potentially lead to significant over- and underpredictions of emissions inventories (up to 20 times), especially in small geographic regions with significant amounts of HDD congestion. However the PAH and *n*-alkane source profiles remained relatively constant for the different modes of operation. Variability of source profiles within the vehicle fleet exceeded the variability due to different operating modes. Analysis of the relative risk associated with the compounds indicated the importance of naphthalene as a significant contributor to the risk associated with diesel exhaust. This high relative risk is driven by the magnitude of the emission rate of naphthalene in comparison to other compounds.

Introduction

Diesel exhaust includes gaseous and particulate phase components. The particulate-phase consists of elemental carbon (EC), organic carbon (OC), trace metals, and other inorganic compounds. OC consists of semivolatile organic compounds (SVOCs) which partition into the particulate or gaseous phase depending on their vapor pressures (10^{-4}−10^{-11} atm). Previous findings have reported concentrations of SVOCs in the gaseous phase to exceed those in the particulate matter (PM) phase by as much as 20 times (*1*). PM emissions arise from within the cylinder of the engine during the combustion process. EC is formed in the center of the fuel spray where the air/fuel ratio is low, while OC results from incomplete or poor combustion of fuel and losses of lubricating oil. As the exhaust cools, SVOCs condense onto the surface of the soot or nucleate to form new particles (*2*).

The organic fraction of diesel exhaust has been found to consist of many known carcinogenic and mutagenic compounds (*3*). Recently, it has been observed that elevated levels of DNA adducts are associated with occupational exposure to diesel PM (*4*, *5*). Ames test results have been used to identify genotoxic and mutagenic compounds found in diesel PM (*4*). In addition to this, in 2002, U.S. EPA reported that diesel PM is carcinogenic (*5*).

Over the past 20 years, numerous researchers have reported that variations of organic composition of gaseous and particulate emissions are attributable to differences in test cycles, fuel composition, engine model year and type, and sampling methodology. Shi et al. (2000) demonstrated that the diesel PM organic fraction increased by more than 2 times from full load to low load, while the EC fraction decreased by a factor of 1.5. Among their findings, they also observed that the fraction of particle-bound PAHs was higher at lower load conditions (*6*).

The work of Schauer et al. (1999) helped demonstrate the importance of sampling methodology when they tested two medium-duty diesel trucks over three different driving cycles (*7*). SVOCs were captured with an annular denuder, followed by a quartz fiber filter, and finally a PUF cartridge. An additional quartz filter (no denuder) collected diesel PM in parallel. The undenuded and denuded filters collected 55 mg and 38 mg of OC, respectively. The difference was determined to be primarily due to the sorption of SVOCs to the undenuded filter and not the vaporization of particulate matter from the filter located downstream of the denuder. Relatively little organic mass was collected on the PUF cartridges located after the filter in the denuder/filter/PUF sampling train.

Lowenthal et al. (1994) developed source profiles for 15 buses and 8 trucks fueled by both diesel no. 2 fuel and Jet A fuel (*8*). Inorganic, bulk carbon, and PAHs were measured and averaged based on vehicle type, fuel type, and emissions control system. The trucks were tested over the Central Business District Cycle (CBD), designed to mimic intracity driving. A total of 18 PAHs were detected in the samples. Total PAH emissions were reported as 13.35 mg mi^{-1}, nearly twice the 6.96 mg mi^{-1} as reported by Schauer et al. (1999) likely attributable to differences in driving cycles, fuels, and vehicle age.

Emission rates of organic species are used in chemical mass balance (CMB) models and emission inventory models. CMB models are important tools to assess the relative contribution of various sources to ambient PM. CMB modeling uses linear combinations of various source profiles to yield a composition equal to that of ambient air (*9*). This type of modeling uses the ratio of chemical species present in order to estimate apportionment of sources. Of critical importance in these models is the proper quantification of the source. A number of researchers have conducted previous studies to initiate these models (*10*−*12*). However, with changes in fuel compositions, engine technologies, and lubricants, these source profiles must be updated. Emission factors are also used in emissions inventory models. Emissions inventory models are based on measurements of emission rates, source activity, and population. For HDD

* Corresponding author phone: (951)781-5695; fax: (951)781-5790; e-mail: dcocker@engr.ucr.edu.
† Department of Chemical and Environmental Engineering.
‡ Bourns College of Engineering.

10.1021/es048086+ CCC: $30.25

Published on Web 06/08/2005

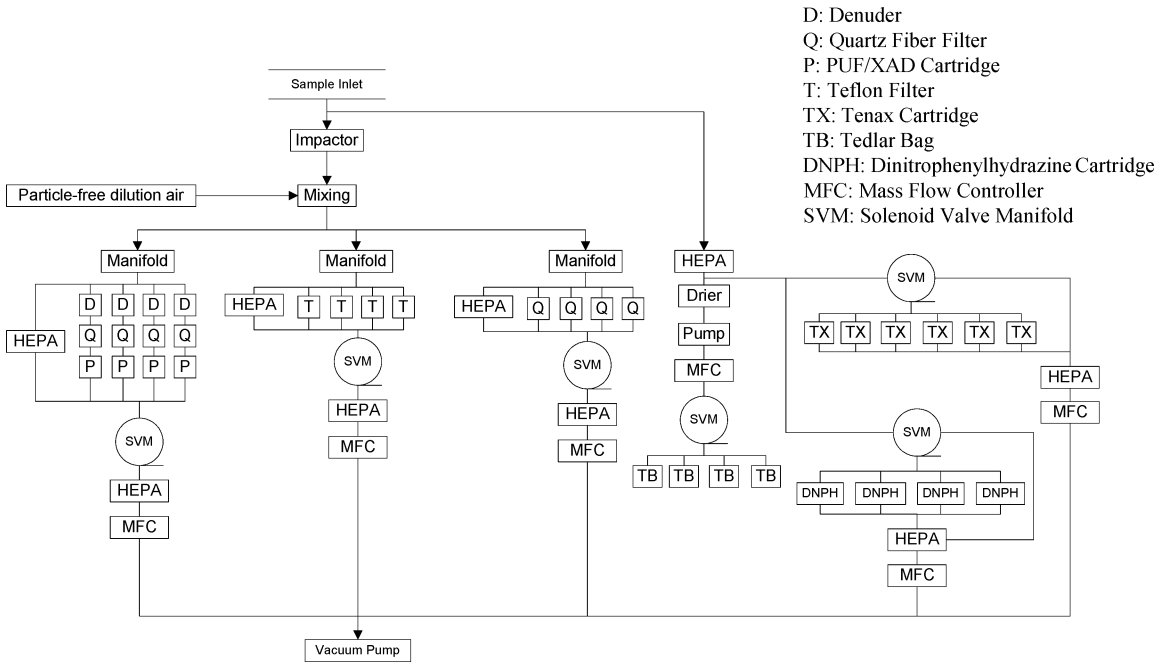

FIGURE 1. Schematic layout of the secondary dilution system.

vehicles, activity measurements can consist of fuel usage, vehicle miles traveled, duration of operation, or power output. These models are dependent on the accuracy of emission rates and can be subject to a certain degree of error due to the dependence of emissions on activity.

The purpose of this work was to quantify the mass emission rates of PAH and *n*-alkane compounds from modern heavy-duty diesel (HDD) engines as they were operated on the road. Vehicles were tested using CE-CERT's on-road Mobile Emissions Laboratory (MEL) over the ARB Four Phase Cycle. The ARB cycle provides the unique opportunity to examine HDD emissions as a function of four distinct operating modes (*13*). A comparison of source profiles, emission rates, and relative toxicity between various vehicles and operating modes are presented here.

Experimental Section

Emissions Testing. Emissions testing of nine HDD vehicles was conducted using CE-CERT's Mobile Emissions Laboratory (MEL). The laboratory is a 53-foot trailer containing a full-scale dilution tunnel, analyzers for gaseous pollutants, a Secondary Dilution System (SDS) for PM samples, and various pumps, compressors, and power supplies necessary to operate the lab. The laboratory can be attached to a HDD vehicle to collect emissions information and samples as the vehicle is driven on the road. PM and SVOC samples are collected using the SDS, designed to meet 2007 CFR specifications for PM sampling. Briefly, the SDS extracts a proportional sample of diluted exhaust from the primary dilution tunnel. As per 2007 CFR (*14*, *15*), the SDS provides the following: removal of particles with an aerodynamic diameter greater than 2.5 μm and temperature control of the filter face to 47 $\pm$ 5 °C. Additionally the SDS provides the capability of collecting parallel sampling trains for PM mass analysis, PM and SVOC organic speciation, Tedlar bags for light hydrocarbon analysis, and DNPH cartridges for aldehydes and ketones analysis. A schematic of the entire SDS sampling system is provided in Figure 1. Further descriptions of the MEL and SDS can be found elsewhere (*16, 17*).

Test Fleet, Fuel, and Test Cycle. The test fleet is summarized in Table 3. Other than changing fuel, all vehicles were tested as-received, and no modifications or maintenance was performed. All vehicles were tested with CARB Ultra-low-sulfur-diesel (sulfur<15 ppm). Typical test fuel properties are listed in Table 4. Vehicles were tested on-road with the vehicle following the speed trace of the ARB Four Phase HDDT Cycle (*13*). This cycle consists of four phases simulating four distinct operating conditions: Cold-Start/Idle, Creep, Transient, and Cruise. Cold-Start/Idle consists of a cold-start of the vehicle followed by a 10 minute idle, Creep simulates heavily congested operation, Transient simulates arterial road driving, and Cruise simulates freeway driving. The speed trace of the test cycle is provided in Figure S1 of the Supporting Information. Testing was conducted at sea level on local roads and Interstate 10 near Coachilla, CA. This area provided a safe area to perform testing with minimum road grade.

TABLE 1. Dionex ASE 200 Operating Parameters

ASE 200 parameter	setpoint
system pressure	14 MPa
oven temperature	100 °C
oven heatup time	5 min
static time	5 min
solvent	methylene chloride
flush volume	60% of extraction cell volume
nitrogen purge	1 MPa for 100 s

TABLE 2. PTV Inlet Operating Parameters

PTV parameter	setpoint
injection volume	20 μL
number of injections	3
delay between injections	40 s
injection time	~1.7 min
vent flow	400 mL min^{-1} until 3.80 min
split flow	500 mL min^{-1} at 6.00 min
gas saver flow	20 mL min^{-1} at 15 min

Sample Media and Analysis. PM samples for chemical analysis were collected on Pall Gelman (Ann Arbor, MI) 47 mm Tissuequartz fiber filters. Prior to sampling, filters were cleaned by baking in a furnace oven at 600 °C for 5 h. Sorbent

TABLE 3. Vehicle Test Fleet

vehicle no.	test date	truck model	odometer (miles)	engine year	engine model	rated power (hp)	speed (rpm)
1	7/20	Freightliner D-120	545 700	1996	Detroit Diesel Series 60	360/400	1800
2	7/29	Freightliner C-120	353 953	1997	Cummins N14	370/435	1800
3	8/14	Freightliner C-120	449 404	1997	Detroit Diesel Series 60	370/430	1800
4	8/17	Freightliner C-120	489 310	1998	Detroit Diesel Series 60	470	2100
5	9/6	Freightliner C-120	469 801	1998	Detroit Diesel Series 60	360	1800
6	12/18	Freightliner C-120	163 349	1998	Detroit Diesel Series 60	370/430	1800
7	1/24	Freightliner C-120	521 048	1998	Caterpillar C-12	355/410	2100
8	1/10	Freightliner C-120	382 246	1999	Caterpillar C-12	355/410	1800
9	9/17	Freightliner C-120	9000	2000	Caterpillar C-15	475	2100

TABLE 4. Typical Properties of CARB Ultralow Sulfur Diesel Fuel Used in This Work

property	test method	limit
ash, wt. %, max	D-482	0.01
carbon residue, 10% btms, wt %, max	D-524	0.35
cetane index, typical	D-4737	55
cetane number, typical	D-613	53.5
Cu strip corr., 3 h @ 122 °F, max	D-130	3
distillation	D-86	
T 90%, °F		540−640
final boiling pt, °F, max		698
flash point, °F, min	D-56	125
gravity, API, typical	D-287	38
lubricity, g, typical	D-6078	3100
stability, mg/100 mL, max	D-2274	1.0
sulfur, ppm	D-5453	15
viscosity, cSt @ 40 °C	D-482	1.9−4.1

TABLE 5. Repeatability of Chemical Speciation from On-Road Testing of a 2000 Freightliner Truck Equipped with a Caterpillar C-15 Engine[a]

	Cold-Start/Idle (%)	Creep (%)	Transient (%)	Cruise (%)
number of samples	4	6	6	6
naphthalene	2.73	8.15	17.7	0.54
acenaphthylene	10.3	22.9	27.4	4.46
acenaphthene	12.1	5.38	25.3	6.54
fluorene	16.4	1.96	50.8	8.59
phenanthrene	32.5	5.12	41.9	5.45
anthracene	26.6	36.6	39.5	17.3
fluoranthene	31.3	8.10	52.6	7.88
pyrene	36.9	8.83	47.4	N/D[a]
benz[*a*]anthracene	33.5	29.6	32.3	9.99
chrysene	31.8	32.1	38.4	34.6
benzo[*b*]fluoranthene	N/D[a]	18.2	47.5	38.9
benzo[*k*]fluoranthene	N/D[a]	23.6	32.4	52.2
benzo[*a*]pyrene	27.4	36.7	31.1	12.8
indeno[1,2,3-*cd*]pyrene	42.5	N/D[a]	22.9	N/D[a]
dibenz[*a,h*]anthracene	10.4	N/D[a]	12.0	41.2
benzo[*ghi*]perylene	58.8	N/D[a]	31.3	N/D[a]
tetradecane	12.3	6.17	12.8	0.93
hexadecane	11.5	3.47	20.8	2.90
octadecane	27.1	11.9	37.4	N/D[a]
nonadecane	24.3	27.1	7.10	3.71
eicosane	45.9	45.6	36.7	N/D[a]
docosane	27.9	10.9	53.6	5.61
tetracosane	16.5	25.4	46.6	13.2
hexacosane	28.2	7.23	45.4	N/D[a]
octacosane	22.9	32.8	51.5	50.8
triacontane	12.4	8.87	69.6	54.9
hexatriacontane	61.4	37.5	48.8	54.9

[a] N/D: not detected.

cartridges consisting of XAD-4 resin in a glass tube, sandwiched by 1.5" polyurethane foam plugs were used to collect SVOC samples. Polyurethane foam plugs, obtained from URG (Chapel Hill, NC), were cleaned by triple sonication in a mixture of hexane, acetonitrile, and methylene chloride (50:30:20) and dried in a vacuum oven. Supelco (Bellefonte, PA) XAD-4 resin was cleaned by methylene chloride extraction in a Dionex (Sunnyvale, CA) Automated Solvent Extractor (ASE 200). All media were stored in a refrigerator at 4 °C after cleaning.

Prior to extraction, collected sample media were spiked with an internal recovery standard consisting of several deuterated species (naphthalene-d_8, acenaphthene-d_{10}, phenanthrene-d_{10}, chrysene-d_{12}, perylene-d_{12}, hexadecane-d_{34}, and tetracosane-d_{50}). Samples were solvent extracted in methylene chloride using the ASE 200. The operating parameters for the ASE 200 are provided in Table 1.

Extracted samples were concentrated to a volume of approximately 5 mL through rotary evaporation using a Buchi Roto-Evaporator. Samples were further concentrated to a volume of 1.5 mL through gentle blowing with purified nitrogen. Extracted, concentrated samples were transferred to amber autoinjector vials for injection into an Agilent 6890N GC equipped with a 5973N MS detector. The GC-MS is equipped with a 0.32 mm i.d., 60 m DB-5ms column, and an Agilent Programmable Temperature Vaporizer (PTV) inlet. The PTV inlet allows for the introduction of a large volume of sample through successive sample injections. Aliquots of sample are injected onto a cooled inlet liner at 35 °C (~100 °C below the lowest boiling point of our compounds of interest), and excess solvent is evaporated in helium. In our current configuration, three successive injections of 20 μL each are made onto a deactivated single baffle liner. This yields a total injection volume of 60 μL, far above the traditional injection volume of 1−2 μL used in most other systems. Table 2 presents the operating parameters of the PTV inlet.

After sample injection, the PTV inlet temperature is ramped to 325 °C at a rate of 720 °C min^{-1}, while the GC oven temperature is maintained at 38 °C. This transfers the entire sample from the inlet liner onto the front of the column. The GC-MS was operated with a temperature profile of the following: hold 5 min at 38 °C, 10 °C min^{-1} to 180 °C, 6 °C min^{-1} to 230 °C, 3 °C min^{-1} to 325 °C, hold 5 min. Column pressure was initially held at 10 psi for 10 min. Following this, the pressure was ramped at a rate of 0.20 psi min^{-1} to 18 psi and held constant until analysis was complete. The MS was operated in scan mode with an 18 min solvent delay. Quantification was performed using a five-point calibration and target ion extraction. The entire method of analysis is based on a modified version of those outlined in EPA Method TO-13A guidelines (*18*).

Field blanks and static blanks of sampling substrates were analyzed to determine the relative mass on clean substrates versus mass on sampled substrates. It was found that blank

TABLE 6. Fleet Averaged Emission Rates of PAHs and *n*-Alkanes

	Idle	Creep	Transient	Cruise
PAH (mg min^{-1})	13.1 ± 12.8	15.5 ± 25.0	86.5 ± 113	18.9 ± 22.4
n-alkane (mg min^{-1})	5.9 ± 9.8	7.7 ± 11.9	30.9 ± 47.4	12.3 ± 22.4
PAH (mg mi^{-1})		528 ± 850	338 ± 441	28.5 ± 33.6
n-alkane (mg mi^{-1})		263 ± 403	121 ± 186	18.5 ± 33.7
PAH (mg (kg of CO_2)$^{-1}$)	331 ± 566	445 ± 794	477 ± 776	103 ± 192
n-alkane (mg (kg of CO_2)$^{-1}$)	242 ± 571	361 ± 821	275 ± 662	74.0 ± 179

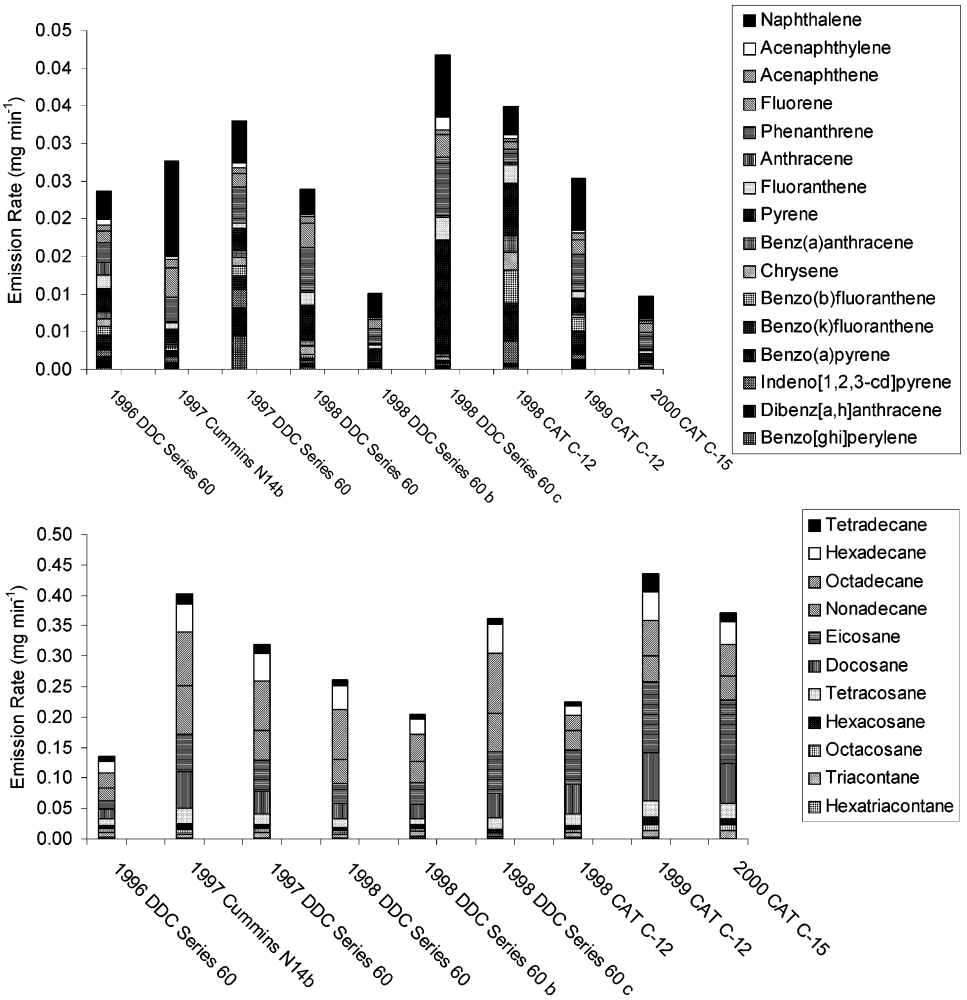

FIGURE 2. PM phase PAH and *n*-alkane emission rates during Cold-Start/Idle.

substrates contained less than 2% (by mass) of the mass typically encountered on sampled substrates. Lower detection limits of the analytical method were determined by examining the level of noise in the vicinity of each target compound. Table S1 of the Supporting Information presents the lower detection limits for each phase of the test cycle. The limits presented in Table S1 are a function of both the sensitivity of the analytical methods and the flow rates utilized during emissions testing. Positive adsorption artifacts for the quartz filters were determined for this sampling system through a comparison of mass collected on parallel quartz filters with one train containing a XAD-4 coated annular denuder upstream of the filter. Mass emission rates reported in this work reflect masses negatively corrected for the adsorption on quartz filters and positively for the PUF/XAD-4 cartridges.

Results and Discussion

Fleet Averaged PAH and *n*-Alkane Emission Rates. Repeat tests of a Freightliner truck equipped with a 2000 Caterpillar C-15 engine were performed on the ARB Four Phase Cycle on 3 nonconsecutive days. The purpose of these tests was to establish the repeatability of PAH and *n*-alkane source signatures from on-road samples. Table 5 presents the coefficient of variation of these tests to demonstrate the ability of the laboratory to produce comparable emission rates for each compound despite testing on several different days with differing ambient conditions. An analysis of variance (ANOVA) test on the average emission rates for each compound over the 3 days shows that these results are statistically similar at 99% confidence level.

Fleet average emission rates (g mi^{-1}, g min^{-1}, and g (kg of CO_2)$^{-1}$) of target PAHs and *n*-alkanes are provided in Table 6. Fleet average emission rates of individual species are provided in Table S2 of the Supporting Information, while emission rates for each vehicle are provided in Table S3. Of particular importance is the standard deviation of the fleet averaged emission rates in Table 6, an indicator of the high variability of emission rates from vehicle to vehicle. Per

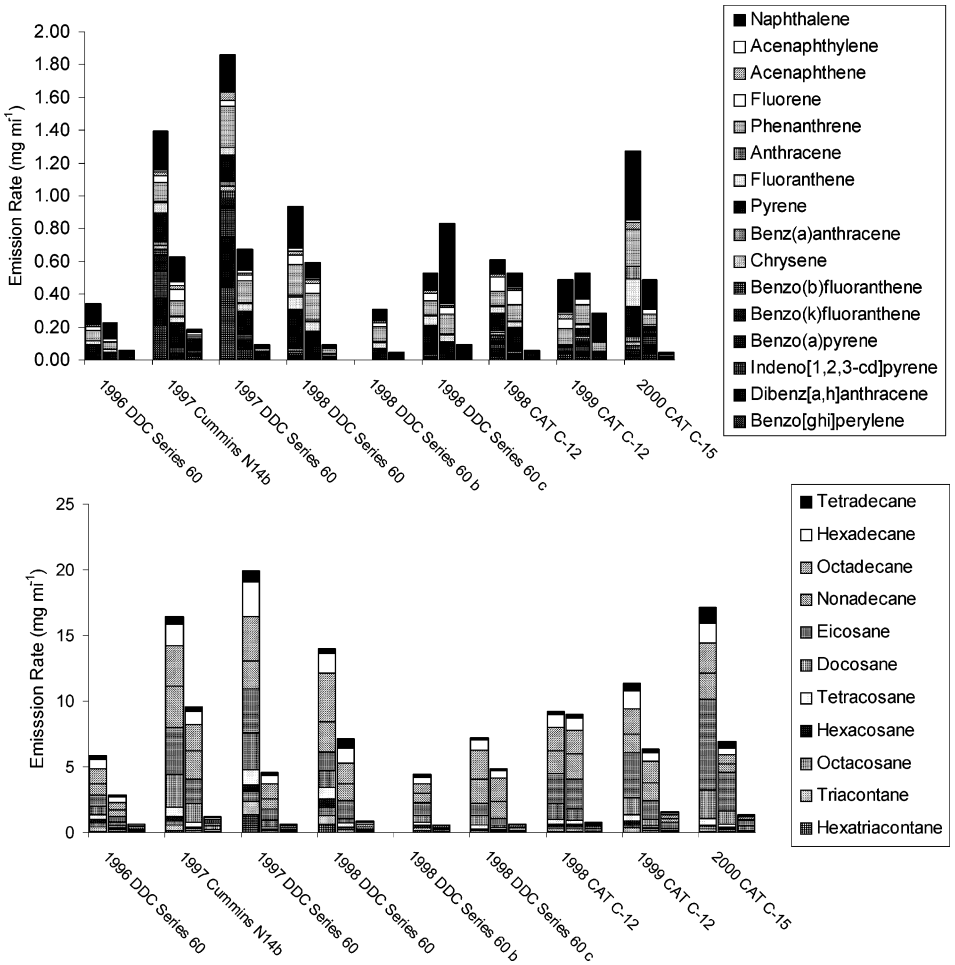

FIGURE 3. Particle phase PAH and *n*-alkane emission rates for nine HDD vehicles. Each set of three columns (from left to right) represents Creep, Transient, and Cruise, respectively.

mile emission rates are highest for Creep > Transient > Cruise.

PAH and *n*-alkane emission rates, normalized by CO_2 production, are also presented in Table 6. CO_2 is a surrogate for fuel consumption and fuel consumed per mile is an indicator of engine activity. Furthermore, normalizing emission rates by CO_2 production allows a comparison of all four phases of the cycle. The difference in fleet average emission rates for different phases of the test cycle is not as pronounced on a per kg of CO_2 basis. This indicates that fuel consumption per mile can explain some of the variability in per mile emission rates between Creep, Transient, and Cruise. However, this does not necessarily imply that PAH and *n*-alkane emissions stem from unburned fuel.

Particle Phase PAH and *n*-Alkane Emission Rates for Individual Vehicles. For this work, the particle-phase is defined as the total mass collected on the quartz filters. Particle phase PAH and *n*-alkane emission rates during Cold-Start/Idle for each vehicle are presented in Figure 2. The average PM phase emission rates of PAHs and *n*-alkanes for Cold-Start/Idle are 25.5 ± 10.6 and 301.5 ± 100.6 ug min^{-1}, respectively. Figure 3 presents the particulate phase PAH and *n*-alkane emission rates of each truck over the three mobile phases of the ARB Four Phase Cycle. Creep phase PAH and *n*-alkane emission rates are greatest followed by Transient and then Cruise, for almost all the test vehicles.

Previously, we demonstrated the variability of elemental and organic carbon emissions with vehicle activity (*19*). The data shown in Figure 3 further demonstrates that PAH and *n*-alkane emission rates vary during different vehicle operating modes. This variation of per mile mass emission rates during different operating modes must be accounted for when conducting emissions inventory models for diesel vehicles.

Although the mass emission rates vary with operating mode, the chemical source profiles of these vehicles are fairly consistent. Figure 4 shows the contribution of each individual species to total particle-phase PAHs and *n*-alkanes. ANOVA analysis of these results shows the profiles to be statistically indistiguishable at the 99% confidence level. An average source profile (in terms of fraction of total PAH or *n*-alkane mass) is provided in Table 7. This source profile is based on the test fleet utilized in this work and may not represent the entire fleet of vehicles on the road. The standard deviations shown in Table 7 may be attributable to variations in the chemical properties of the lubricating oil in each vehicle.

Total PAH and *n*-Alkane Emission Rates for Individual Vehicles. Total PAH and *n*-alkane emission rates (defined as the sum of the mass collected on the quartz filters and PUF/XAD cartridges) for Cold-Start/Idle and the mobile phases of the ARB Four Phase Cycle are shown in Figures 5 and 6. The SVOC fraction (collected on PUF/XAD cartridges) contributes a significant portion of the total mass of PAHs and *n*-alkanes. During the Cold-Start/Idle, naphthalene emission rates are several orders of magnitude greater than other compounds, while *n*-alkane emissions are dominated by tetradecane, hexadecane, and octadecane. During the mobile phases of the ARB Four Phase Cycle, naphthalene is still a dominant species for each vehicle, but the presence of other species can be seen. As in the Cold-Start/Idle, the

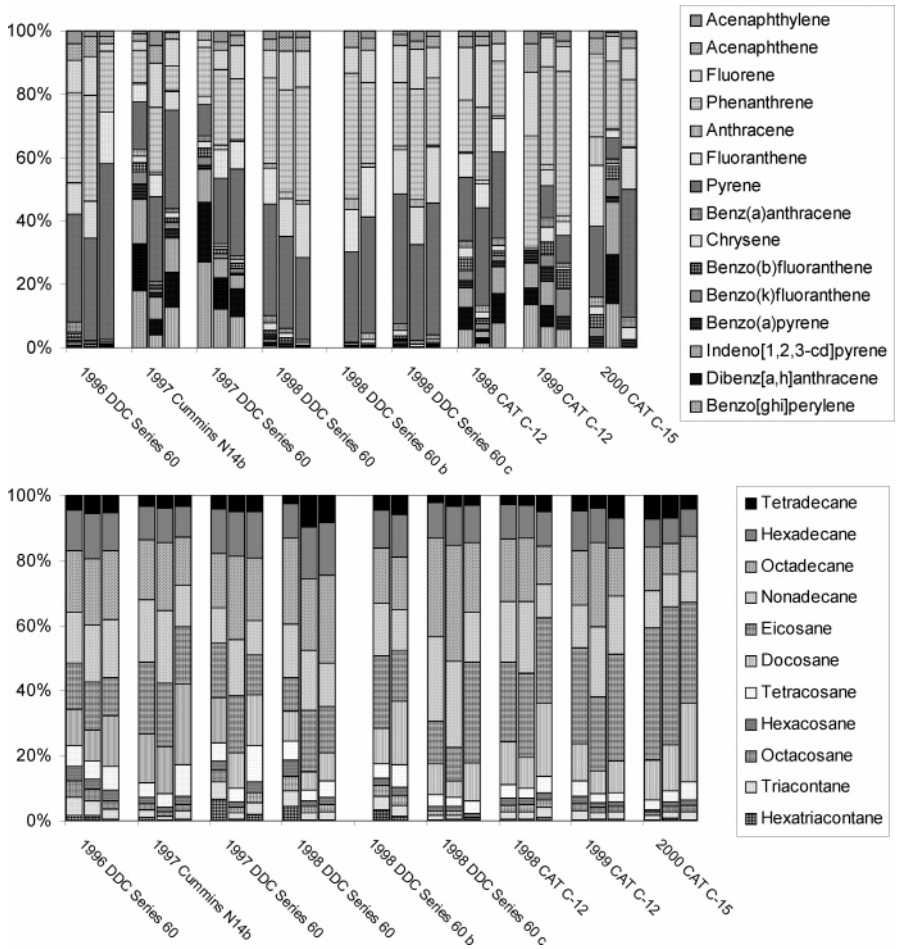

FIGURE 4. Relative contribution of each species in the PM phase to total mass of PAHs and *n*-alkanes in the PM phase. Each set of three columns (from left to right) represents Creep, Transient, and Cruise, respectively.

TABLE 7. Average Percent Contribution of Each Chemical Species in the Particulate Phase to the Total Mass of Reported PAHs and Reported *n*-Alkanes in the Particulate Phase

	Creep (%)	Transient (%)	Cruise (%)
	PAHs		
naphthalene	24.5 ± 10.8	29.6 ± 14.9	25.2 ± 20.8
acenaphthylene	1.45 ± 0.849	1.61 ± 1.09	1.15 ± 0.661
acenaphthene	3.14 ± 1.05	2.37 ± 1.34	2.28 ± 1.08
fluorene	6.64 ± 4.99	8.27 ± 4.01	6.15 ± 2.98
phenanthrene	16.1 ± 4.06	18.9 ± 4.54	16.3 ± 7.43
anthracene	1.19 ± 2.00	0.891 ± 0.511	0.537 ± 0.329
fluoranthene	6.56 ± 4.34	5.76 ± 2.58	8.67 ± 4.13
pyrene	16.8 ± 10.4	16.4 ± 7.87	24.5 ± 11.7
benz[*a*]anthracene	1.57 ± 0.661	1.06 ± 0.601	1.16 ± 0.775
chrysene	1.41 ± 0.867	1.05 ± 1.04	1.13 ± 0.948
benzo[*b*]fluoranthene	1.72 ± 1.24	1.31 ± 1.01	0.941±0.857
benzo[*k*]fluoranthene	1.42 ± 1.26	1.27 ± 1.22	1.14 ± 1.26
benzo[*a*]pyrene	1.66 ± 1.27	0.901 ± 1.12	1.08 ± 0.978
indeno[1,2,3-*cd*]pyrene	4.08 ± 4.48	3.45 ± 3.75	2.67 ± 3.89
dibenz[*a,h*]anthracene	5.05 ± 6.19	3.53 ± 3.82	3.30 ± 4.46
benzo[*ghi*]perylene	6.53 ± 8.68	3.51 ± 4.03	3.71 ± 4.66
	Alkanes		
tetradecane	3.95 ± 1.63	5.17 ± 2.25	5.15 ± 1.77
hexadecane	11.1 ± 1.49	11.8 ± 2.62	11.4 ± 2.72
octadecane	20.1 ± 5.58	22.5 ± 7.34	17.6 ± 5.49
nonadecane	16.3 ± 4.91	19.3 ± 4.86	13.5 ± 3.31
eicosane	21.3 ± 10.0	21.6 ± 9.67	22.0 ± 9.14
docosane	11.9 ± 2.06	9.50 ± 3.55	16.6 ± 6.45
tetracosane	4.79 ± 1.23	3.61 ± 0.899	6.27 ± 2.94
hexacosane	2.53 ± 1.42	1.78 ± 0.544	2.23 ± 0.856
octacosane	2.75 ± 1.49	1.90 ± 0.761	2.02 ± 0.757
triacontane	3.19 ± 1.71	2.19 ± 1.03	2.45 ± 0.967
hexatriacontane	1.90 ± 2.38	0.641 ± 0.468	0.729 ± 0.525

n-alkane emissions are dominated by tetradecane, hexadecane, and octadecane. The fraction of mass collected on the PUF/XAD cartridges was 10−1000 times higher than that collected in the PM phase. The difference is predominantly driven by naphthalene, most of whose mass was found in the gas phase. The presence of more mass in the gaseous phase over the PM phase is similar to results seen in other work, but the magnitude of the difference is greater here (*1*, *7*). An important caveat to note is the difference in sampling conditions. As specified in the CFR, the SDS used for sampling PM and SVOCs maintains the sample temperature at 47 ± 5 °C. Results reported by other researchers may have utilized different sampling temperatures than those used here, thus influencing the gas to particle partitioning (affected by temperature, concentration, and vapor pressure) (*20*).

Comparison of Emission Rates. To determine the effects of operating mode on emissions, a ratio of per mile emission rates can be calculated as

$$\text{ratio}_{ij} = \frac{\text{emission rate mode i}}{\text{emission rate mode j}} \quad (1)$$

Table 8 presents the ratio of emission rates for select metrics between Creep, Transient, and Cruise. The ratio of fuel consumption is also shown to demonstrate that these trends hold after normalization for fuel consumed. These data indicate that per mile emission rates of PAHs and *n*-alkanes during congested conditions are approximately an order of magnitude higher than cruising conditions.

Analysis of Relative Risk Associated with Emissions. Inhalation unit risk factors for cancer are available for several of the compounds detected in this work (*21*). Table 9 presents a summary of the available unit risk factors. Typically, these risk factors are multiplied by the concentration of a particular

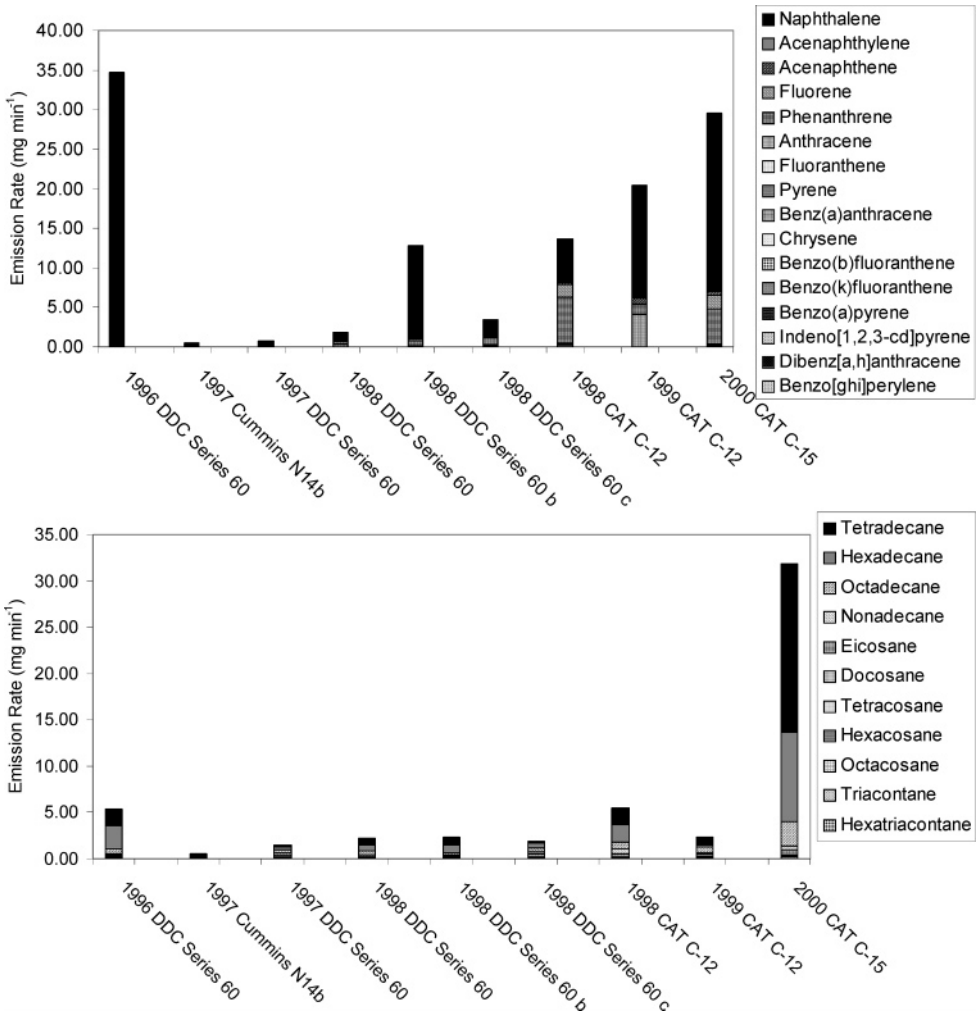

FIGURE 5. Total PAH and *n*-alkane emission rates for nine trucks during Cold-Start/Idle.

TABLE 8. Comparison of per Mile Fleet Averaged Emission Rates between Different Operating Modes

	Creep:Transient	Creep:Cruise	Transient:Cruise
total BaP	5.0	14.1	2.8
total PAHs	1.6	18.4	11.9
particle phase PAHs	1.5	8.3	5.5
n-alkanes	2.1	13.7	6.5
organic carbon[a]	3.4	8.1	2.4
elemental carbon[a]	0.76	1.9	2.5
particulate matter[a]	1.5	3.5	2.3
fuel	1.9	2.8	1.5

[a] Reference *19*.

species in the ambient air, to yield a cancer risk for the population. Here, we present the relative risk associated with each chemical species as the product of its emission rate (μg mi^{-1}) and the unit risk factor (μg m^{-3})$^{-1}$. The resulting value allows for a direct comparison of relative risk associated with each species. The relative risk values can be ranked by normalizing with the highest value of relative risk (in this case, naphthalene during Creep) to yield a measure of the importance of various species. For example, a normalized value of 0.1 means that the relative risk for the species indicated is 10 times lower than that for naphthalene during the creep phase. Table 10 presents normalized relative risk calculated for the fleet averaged emission rates. Several gas-phase air toxics are also included in Table 10 for comparison (*22*).

Relative risk associated with the Creep phase of the ARB Four Phase Cycle was 8−23 times higher than that associated with the Cruise phase. This implies that communities that are impacted by their close proximity to areas subject to congested HDD traffic conditions are at considerably higher risk per vehicle transiting the area for the compounds with unit risk factors reported in this paper. The importance of naphthalene as a contributor to relative risk can be seen in Table 10. Although the unit risk factor for naphthalene is at least an order of magnitude lower than other species, the magnitude of its emission rate makes it the most significant contributor to the relative risk from individual species with unit risk factors reported in this paper. Relative risk associated with naphthalene is approximately 3 orders of magnitude higher than any of the chemical species found in the PM phase. It should be noted that there are many compounds in diesel exhaust with inhalation unit risk factors larger than those examined here (nitro-PAHs, quinones, di-nitro-PAHs, metals, and metal oxides). However, previous research has shown that the emission rates of these compounds are much lower than that of PAHs, and thus it is expected that the contribution of these compounds will not be significant. As previously reported, other gas-phase air toxics (acetaldehyde, 1,3-butadiene, etc.) are not significant contributors to the relative risk associated with diesel exhaust (*22*).

Discussion

The variation of PAH and *n*-alkane emissions due to changes in vehicle activity and vehicle-to-vehicle variations has important implications on emissions modeling. Models used

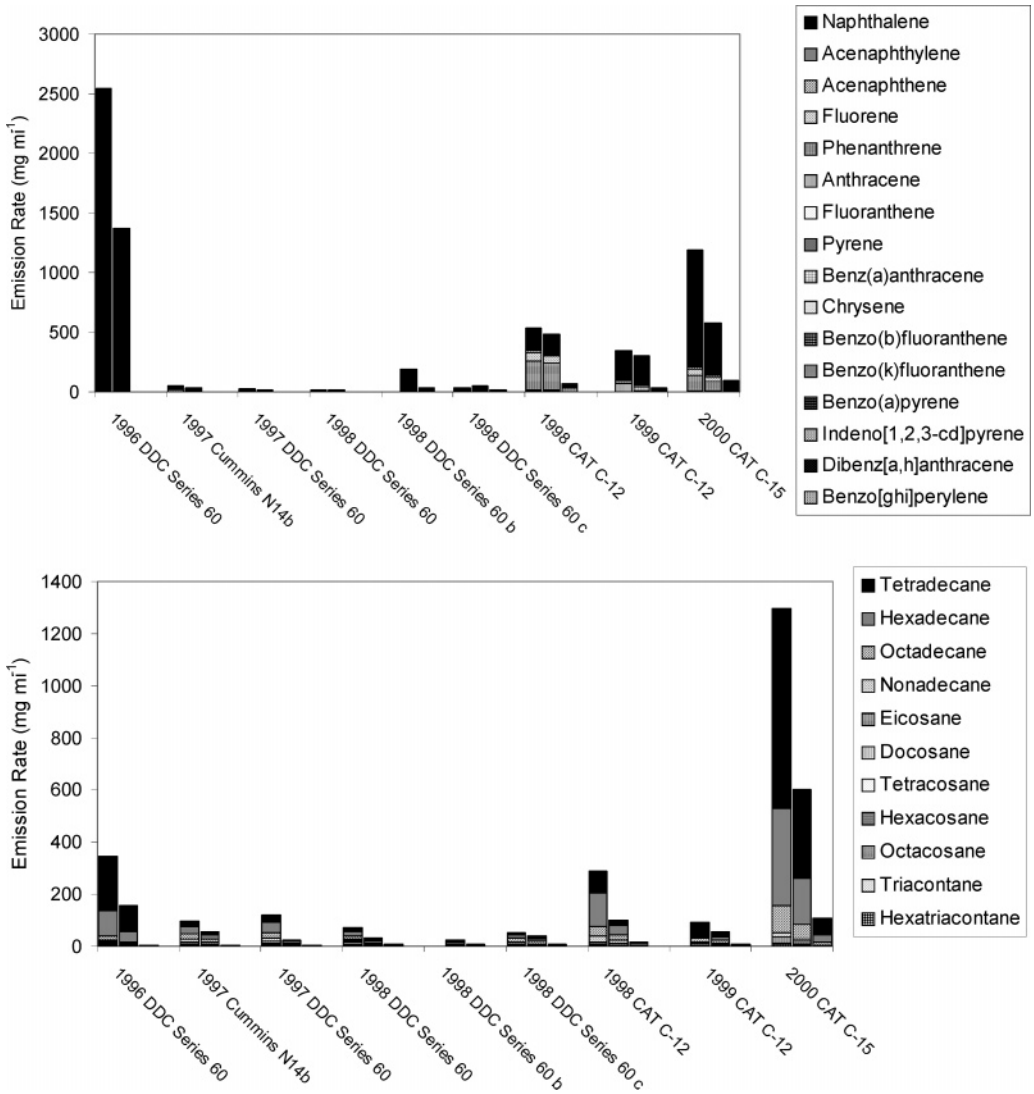

FIGURE 6. Total PAH and *n*-alkane emission rates for nine HDD vehicles. Each set of three columns (from left to right) represents Creep, Transient, and Cruise, respectively.

TABLE 9. Summary of Inhalation Unit Risk Factors (*21*)

chemical	inhalation unit risk (μg m^{-3})$^{-1}$
naphthalene	3.40E−05
benz[*a*]anthracene	1.10E−04
chrysene	1.10E−05
benzo[*b*]fluoranthene	1.10E−04
benzo[*k*]fluoranthene	1.10E−04
benzo[*a*]pyrene	1.10E−03
indeno[1,2,3-*cd*]pyrene	1.10E−04
dibenz[*a,h*]anthracene	1.20E−03

to perform emissions inventory estimates must account for vehicle activity, traffic density, and population makeup (traffic based modeling). Failure to properly characterize the source site can lead to significant over- and underpredictions in model estimates. This is especially important for modeling emissions in small urban regions.

We have previously shown that the elemental and organic carbon (EC and OC) emission rates also vary with operating mode (*19*). CMB models that attempt to use a combination of chemical source profiles and EC must account for vehicle operating modes, as EC does not exhibit proportional changes with carbon dioxide.

TABLE 10. Fleet Averaged Relative Risk Factors

	Creep	Transient	Cruise
naphthalene	1.00	0.62	0.045
benz[*a*]anthracene	0.00021	0.00017	0.00002
chrysene	0.000025	0.000025	0.0000027
benzo[*b*]fluoranthene	0.00014	0.000054	0.000011
benzo[*k*]fluoranthene	0.00011	0.000052	0.000014
benzo[*a*]pyrene	0.0019	0.00038	0.00014
indeno[1,2,3-*cd*]pyrene	0.00032	0.00013	0.000023
dibenz[*a,h*]anthracene	0.0051	0.00159	0.00029
acetaldehyde[a]	0.000051	0.000015	0.000002
benzene[a]	0.000057	0.000012	0.000004
1,3-butadiene[a]	0.000286	0.000061	0.000019
formaldehyde[a]	0.000299	0.000091	0.000015

[a] Ref *22*.

Relative risk calculated for several of our target compounds showed the importance of the gaseous/SVOC fraction as a contributor to the risk associated with diesel exhaust. This finding was made possible by the recent adoption of an inhalation unit risk factor for naphthalene. This highlights the need to evaluate the gaseous fraction as part of health risk assessments as its contribution to the relative risk is far greater than that of the PAHs found in the PM phase. The

process of health risk assessment is constantly evolving. As inhalation unit risk factors are adopted for other compounds these assessments must be re-evaluated. Current health risk assessments identify diesel PM as the primary source of carcinogenic end effects. We have seen here that the gaseous fraction can also be a significant contributor. Prior to the adoption of a unit risk factor for naphthalene, the end effects of the gaseous/SVOC fraction of diesel exhaust were not accounted for in health risk assessments. With this new knowledge of the magnitude of on-road emission rates of SVOC species and the cancer risk associated with these species, health risk assessments for exposure to diesel exhaust must be re-evaluated on a basis of exposure to whole exhaust, not just diesel PM.

Acknowledgments

The authors would like to thank Joseph M. Norbeck for his helpful comments and insight throughout the course of this research. We would also like to thank Kent C. Johnson and Don Pacocha of CE-CERT's Mobile Emissions Laboratory for their assistance in vehicle testing and Kathalena Cocker for her assistance in analytical analysis of samples. Funding for this work was provided in part by California Air Resources Board, Strategic Environmental Research and Development Program, U.S. EPA and Cummins Incorporated.

Supporting Information Available

The ARB Four Phase Cycle of Cold-Start/Idle (I), Creep (II), Transient (III), and Cruise (IV) phases (Figure S1), lower detection limits for PAHs and *n*-alkanes during this test campaign (Table S1), fleet averaged emission rates of individual organic species over the ARB Four Phase Cycle (Table S2), and PAH and *n*-alkane emission rates of individual vehicles (Table S3). This material is available free of charge via the Internet at http://pubs.acs.org.

Literature Cited

(1) Gartziandia, E. L.; Tatry, V.; Carlier, P.; Sampling and Analysis of Organic Compounds in Diesel Particulate Matter. *Environ. Monit. Assess.* **2000**, *65*, 155−163.

(2) Yanowitz, J.; McCormick, R. L.; Graboski, M. S. In-Use Emissions from Heavy-Duty Diesel Vehicles. *Environ. Sci. Technol.* **2000**, *5*, 729−740.

(3) Health Effects Institute. *Diesel Exhaust: A Critical Analysis of Emissions, Exposure, and Health Effects;* 1995.

(4) Lloyd, A. C.; Cackette, T. A.; Diesel Engines: Environmental Impact and Control. *J. Air Waste Manage.* **2001**, *51*, 809−847.

(5) U.S. Environmental Protection Agency. *Health Assessment Document for diesel engine Exhaust*, Prepared by the National Center for Environmental Assessment, Washington, DC, for the Office of Transportation and Air Quality, 2002; EPA/600-8-90-057F.

(6) Shi, J. P.; Mark, D.; Harrison, R. M. Characterization of Particles from a Current Technology Heavy-Duty Diesel Engine. *Environ. Sci. Technol.* **2000**, *34*, 748−755.

(7) Schauer, J. J.; Kleeman, M. J.; Cass, G. R.; Simoneit, B. R. T. Measurement of Emissions from Air Pollution Sources. 2. C1 Through C30 Organic Compounds from Medium Duty Diesel Trucks. *Environ. Sci. Technol.* **1999**, *33*(10), 1578−1587.

(8) Lowenthal, D. H.; Zielinska, B.; Chow, J. C.; Watson, J. G.; Gautam, M.; Ferguson, D. H.; Neuroth, G. R.; Stevens, K. D. Characterization of Heavy-Duty Diesel Vehicle Emissions. *Atmos. Environ.* **1994**, *28*(4), 731−743.

(9) Schauer, J. J.; Cass, G. R. Source Apportionment of Wintertime Gas-Phase and Particle-Phase Air Pollutants Using Organic Compounds as Tracers; *Environ. Sci. Technol.* **2000**, *34*, 1821−1832.

(10) Li, C. K.; Kamens, R. M. The Use of Polycyclic Aromatic Hydrocarbons as Source Signatures in Receptor Modeling. *Atmos. Environ.* **1993**, *274*(4), 523−532.

(11) Khalili, N. R.l Scheff, P. A.; Holsen, T. M., PAH Source Fingerprints for Coke Ovens, Diesel and Gasoline Engines, Highway Tunnels, and Wood Combustion Emissions. *Atmos. Environ.* **1995**, *29*(4), 533−542.

(12) Schauer, J. J.; Rogge, W. F.; Hildeman, L. M.; Mazurek, M. A.; Cass, G. R.l Simoneit, B. R., Source Apportionment of Airborne Particulate Matter Using Organic Compounds as Tracers. *Atmos. Environ.* **1996**, *30*(22), 3837−3855.

(13) Gautam, M.; Clark, N.; Riddle, W.; Nine, R.; Wayne, W. S.; Maldonado, H.; Agrawal, A.; Carlock, M. Development and Initial Use of a Heavy-Duty Diesel Truck Test Schedule for Emissions Characterization. *SAE Technical Paper Series;* 2002; 2002-01-1753.

(14) Code of Federal Regulations. *Protection of the Environment,* 40 CFR 86.1312

(15) Code of Federal Regulations. *Protection of the Environment,* 40 CFR 86.1310

(16) Cocker, D. R.; Johnson, K. J.; Shah, S. D.; Miller, J. W.; Norbeck, J. M. Development and Application of a Mobile Laboratory for Measuring Emissions From Diesel Engines I. Regulated Gaseous Emissions. *Environ. Sci. Technol.* **2004**, *38*, 2182−2189.

(17) Cocker, D. R.; Shah, S. D.; Johnson, K. J.; Zhu, X.; Miller, J. W.; Norbeck, J. M. Development and Application of a Mobile Laboratory for Measuring Emissions From Diesel Engines II. Particulate and Non-Regulated Emissions. *Environ. Sci. Technol.* **2004**, in press.

(18) U.S. EPA. Compendium Method TO-13A, Determination of Polycyclic Aromatic Hydrocarbons (PAHs) in Ambient Air Using Gas Chromatography/Mass Spectrometry (GC/MS), Office of Research and Development, January 1999.

(19) Shah, S. D.; Cocker, D. R.; Miller, J. W.; Norbeck, J. M. Emission Rates of Particulate Matter and Elemental and Organic Carbon from In−Use Diesel Engines. *Environ. Sci. Technol.* **2004**, *38*, 2544−2550.

(20) Mader, B. T.; Pankow, J. F. Gas/Solid Particle Partitioning of Semivolatile Organic Compounds (SOCs) to Air Filters. 3. An Analysis of Gas Adsorption Artifacts in Measurements of Atmospheric SOCs and Organic Carbon (OC) when using Teflon Membrane Filters and Quartz Fiber Filters. *Environ. Sci. Technol.* **2001**, *35*(17), 3422−3432.

(21) California Air Resources Board Consolidated Table of OEHHA/ARB Approved Risk Assessment Health Values Last Update: August 23, 2004.

(22) Zhu, X. A Quantitative Assessment of the Impact of Gas-Phase Toxic Emissions from Motor Vehicles on Public Health and Welfare, Ph.D. Thesis, University of California, Riverside.

Received for review December 3, 2004. Revised manuscript received March 30, 2005. Accepted May 5, 2005.

ES048086+